photonics

MDPI

Communication

Radiophotoluminescence Phenomenon of CaF_2 Ceramics Doped with Li

Takumi Kato, Daisuke Nakauchi, Noriaki Kawaguchi and Takayuki Yanagida *

Division of Materials Science, Graduate School of Science and Technology, Nara Institute of Science and Technology, 8916-5 Takayama, Ikoma, Nara 630-0192, Japan
* Correspondence: t-yanagida@ms.naist.jp

Abstract: The objective of this study is to examine the impact of Li-doping on the radiophotoluminescent (RPL) properties of CaF_2. Before ionizing irradiation, Li-doped CaF_2 exhibited no photoluminescence (PL) under excitation in the range of 250–700 nm. After ionizing irradiation, Li-doped CaF_2 displayed PL at 800 nm when excited at 390 and 610 nm. The decay time constant for this luminescence was determined to be 20 ns, which suggests that it is attributed to $(F_2^+)_A$ centers. All the Li-doped CaF_2 showed higher PL intensity than the non-doped CaF_2 did, with the highest intensity observed in the 0.5% Li-doped CaF_2. The 0.5% Li-doped CaF_2 was also found to have a minimum measurable dose of 14 μGy as an RPL dosimeter, and the RPL response monotonically increased to 10 Gy. As for radiation-induced luminescence other than RPL, the scintillation peak and the thermally stimulated luminescence (TSL) glow peak were mainly observed at 300 nm and 140 °C, respectively.

Keywords: radiophotoluminescence; CaF_2; dosimeter

Citation: Kato, T.; Nakauchi, D.; Kawaguchi, N.; Yanagida, T. Radiophotoluminescence Phenomenon of CaF_2 Ceramics Doped with Li. *Photonics* **2023**, *10*, 211. https://doi.org/10.3390/photonics10020211

Received: 28 December 2022
Revised: 8 February 2023
Accepted: 14 February 2023
Published: 15 February 2023

1. Introduction

Radiophotoluminescence (RPL) is categorized as one aspect of storage luminescence that is commonly used in dosimetry [1]. The process of achieving RPL involves the generation of new photoluminescence (PL) centers through ionizing irradiation. As the intensity of luminescence from these newly created PL centers increases in response to increasing doses of radiation, RPL materials are well-suited for dosimetric applications. Thermally and optically stimulated luminescence (TSL and OSL) are also categorized as storage luminescence. In these phenomena, electron-hole pairs created by ionizing irradiation are temporarily accumulated at trapping centers. These electron-hole pairs are subsequently de-trapped by external stimulation (such as heat or light) and then recombine on luminescence centers. TSL and OSL materials are also useful in dosimetry, particularly in imaging plates and personal dosimeters [2,3]. Compared to TSL and OSL, RPL materials have the advantage of being able to observe radiation doses without the fading of electron-hole pairs [4,5]. This makes RPL a valuable tool in the field of dosimetry.

There are two main categories of RPL materials, which are classified based on PL centers. The first category, known as activator-based RPL materials, includes materials such as Ag-doped phosphate glass [6–12], Cu-doped aluminoborosilicate glass [13], Eu-doped materials [14–17], and Sm-doped materials [18–20]. The second category, known as lattice-defect-based RPL materials, includes materials such as C- and Mg-codoped Al_2O_3 [21–23], LiF [24], MgF_2 [25], K_2CO_3 [26], and Na_2CO_3 [27]. These materials exhibit RPL phenomena due to the generation of anion defects such as in the F_2 and F_2^+ centers in C- and Mg-codoped Al_2O_3.

CaF_2 is a versatile material that has been used in a variety of applications, including as a dosimeter for measuring radiation exposure. One particularly interesting property of CaF_2 is its ability to exhibit RPL when doped with certain rare-earth ions. For example,

when doped with Eu, CaF_2 exhibits RPL based on valence modification between trivalent and divalent states [17,28]. On the other hand, CaF_2 has been doped with Dy, Tm, or Mn to be used as a TSL dosimeter (TLD-200, 300, and 400, respectively) for a long time [29–34]. Moreover, rare-earth or transition-metal-doped CaF_2 has shown OSL [35–37]. More recently, we have discovered that non-doped CaF_2 also shows RPL arising from the F_2^+ and $(F_2^+)_A$ centers [38,39]. The F_2^+ center is formed by the aggregation of two anion defects capturing an electron, and it can change to the $(F_2^+)_A$ center when an impurity is present nearby, i.e., it is a $(F_2^+)_{Na}$ center when a Na impurity is present nearby [40,41]. In addition, our previous study revealed that the RPL response was improved by Na-doping in CaF_2 [42].

In this research, we examined the impact of Li-doping on the RPL properties of CaF_2. As the valence of Li is similar to that of Na, it is believed that monovalent ions such as Li will boost the RPL response. This is because the charge compensation between Li^+ and Ca^{2+} ions creates anion defects in CaF_2, which leads to increased RPL intensity. Furthermore, we measured scintillation spectra and TSL glow curves, which are categorized as radiation-induced luminescence.

2. Materials and Methods

In a previous study, we utilized spark plasma sintering (SPS) equipment (LabX-100, Sinter Land, Kyoto, Japan) to prepare CaF_2 ceramics [38]. In this study, we employed the same method and conditions to prepare Li-doped CaF_2 transparent ceramics. CaF_2 (5N, Stella Chemifa, Osaka, Japan) and LiF (4N, Stella Chemifa) were used as reagent powders, and LiF was doped in CaF_2 at a molar ratio of 0.01, 0.05, 0.1, 0.5, and 1 mol%.

The RPL properties of the CaF_2 ceramics doped with Li were investigated below. PL excitation/emission maps were recorded with Quantaurus-QY (C11347-01, Hamamatsu, Shizuoka, Japan). In this measurement, PL emission spectra were recorded in the excitation range from 250 to 700 nm with a 10 nm interval. In order to evaluate a dose response property, the PL emission spectra were measured using a spectrofluorometer (FP-8600, JASCO) after the Li-doped CaF_2 ceramics were irradiated by X-rays with several doses (from 0.01 mGy to 10 Gy). The PL decay time profile was recorded by Quantaurus-τ (C11367, Hamamatsu), and then the decay time constant was calculated from the least-square fitting by some exponential decay functions.

In addition to RPL properties, the scintillation spectra and TSL glow curves were measured by our original setup [43] and a TSL reader (TL-2000, Nanogray, Osaka, Japan) [44], respectively. In this study, the radiation source was an X-ray generator (XRB80P&N200 × 4550, Spellman, Houston, TX, USA) [45]. The applied voltage was fixed to 40 kV (DC) while the tube current varied from 0.052 to 5.2 mA to control the dose rate, and the mean X-ray energy was 26 keV. The irradiated dose was calibrated using an air-filled ionization chamber (TN30013, PTW, Freiburg im Breisgau, Germany), and the dose was defined as dose in-air delivered at the entrance of the sample.

2.1. Sample

Figure 1 indicates the appearance of the Li-doped CaF_2 ceramics under light from a fluorescent lamp and UV lamp (365 nm) before and after ionizing irradiation. The thickness and diameter of the Li-doped CaF_2 ceramics were 0.8 and 10 mm, respectively. The Li-doped CaF_2 ceramics initially appeared colorless and translucent under the light from the fluorescent lamp and did not exhibit any luminescence under the light from the UV lamp. On the other hand, the radiation-irradiated ceramics underwent a transformation, displaying a blue coloration and emitting red luminescence under UV light. These observations are consistent with those made in the previous study on CaF_2 ceramics doped with Na^+ ions, providing further evidence for the production of PL centers in CaF_2 ceramics through ionizing irradiation [42].

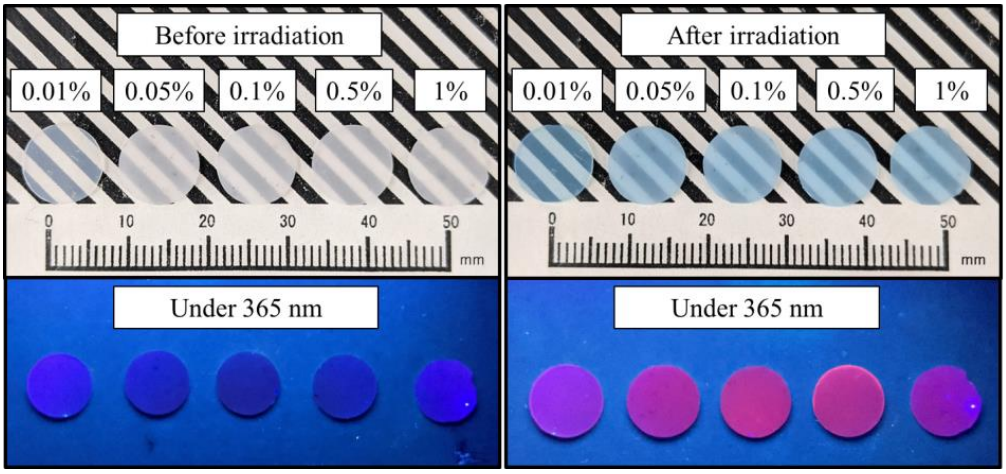

Figure 1. Appearance of the Li-doped CaF_2 ceramics under light from the fluorescent lamp and UV lamp (365 nm) before and after ionizing irradiation.

2.2. RPL Properties

Figure 2 shows the PL excitation/emission maps of the 0.5% Li-doped CaF_2 ceramic (a) before and (b) after ionizing irradiation. Although the 0.5% Li-doped CaF_2 ceramic before ionizing irradiation showed no emission signals, an emission band at approximately 800 nm under excitations at 390 and 610 nm was detected after ionizing irradiation. Our past studies revealed that these emission bands were caused by $(F_2^+)_A$ centers [38,39]. Additionally, this emission band was also detected in other Li-doped samples. On the other hand, the emission band originating from F_2^+ centers was not observed in the Li-doped CaF_2 ceramics unlike in the non-doped and Na-doped ones [38,42]. These results imply that the generation of F_2^+ and $(F_2^+)_A$ centers may be independent events, and that $(F_2^+)_A$ centers can become RPL centers without the existence of F_2^+ centers.

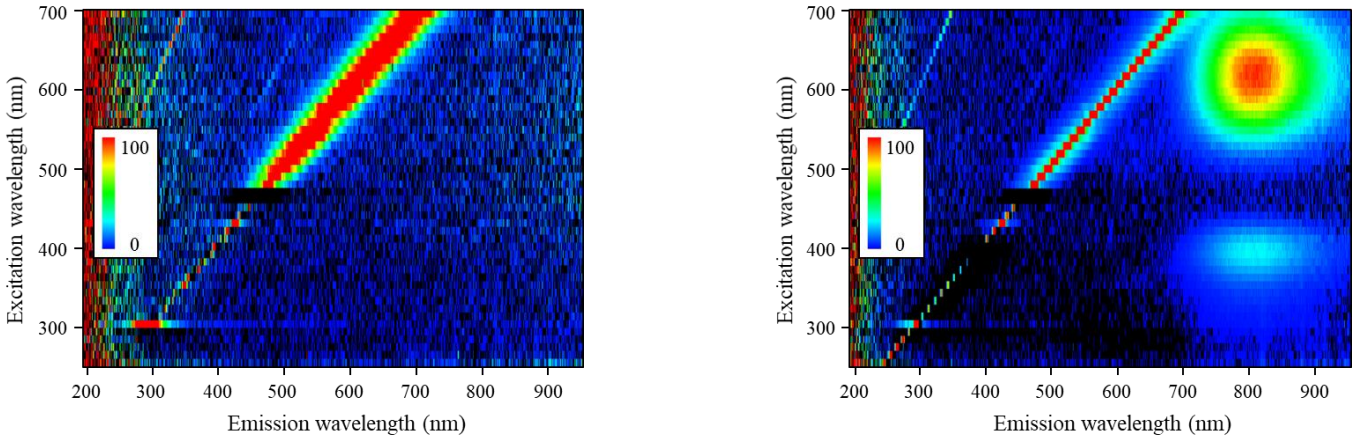

Figure 2. PL excitation/emission maps of the 0.5% Li-doped CaF_2 ceramic (**a**) before and (**b**) after ionizing irradiation. The horizontal and vertical axes indicate emission and excitation wavelengths, respectively.

The PL decay time profile of the 0.5% Li-doped CaF_2 ceramic, as a representative of all the samples after ionizing irradiation, is illustrated in Figure 3. A single exponential decay function was utilized to reproduce the PL decay time profile with a decay time constant of 20 ns. This value is approximately consistent with the decay time constant of

non-doped CaF_2 [39], indicating that the decay time constant is related to the presence of $(F_2^+)_A$ centers.

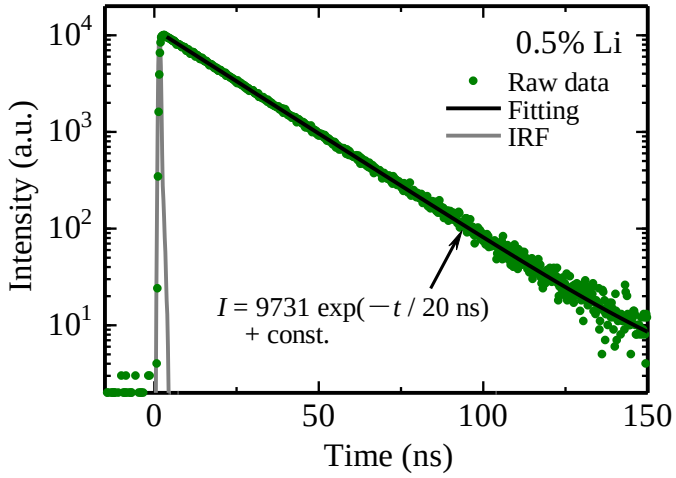

Figure 3. PL decay time profile of the 0.5% Li-doped CaF_2 ceramic after ionizing irradiation (10 Gy). The excitation and monitored wavelengths are 630 and 760 nm, respectively. IRF stands for instrumental response function.

Figure 4 shows the PL spectra of the Li-doped CaF_2 ceramics under 640 nm excitation. An emission peak was detected at around 760 nm. This wavelength was shorter than that observed in Figure 2 and slightly differed from our previous results [39,42]. This difference was due to the difference in the measurement methods. For example, when comparing the measurements of reflective and transmissive types, the transmissive type is strongly affected by self-absorption. As a result, the emission wavelength may shift to a side with a longer wavelength in the case that the emission wavelength is close to the excitation wavelength. PL excitation/emission maps (Figure 2) were measured by the transmissive-type device. On the other hand, PL spectra (Figure 4) were measured by the reflective-type device. This difference would cause a different peak-top.

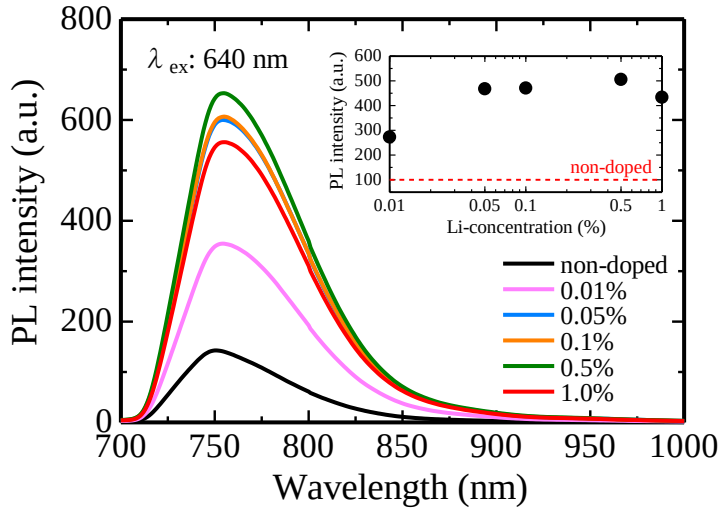

Figure 4. PL spectra of the Li-doped CaF_2 ceramics and the reference sample (non-doped CaF_2) [39]. The inset shows the correlation between the PL intensity and Li-concentration in CaF_2 ceramics.

The graph in the inset illustrates the correlation between the PL intensity and Li-concentration in CaF_2 ceramics. Here, the PL spectrum measured by the same condition of the non-doped ceramics was included for comparison [39]. It was observed that the

PL intensity was enhanced by the presence of Li-doping. All the Li-doped CaF_2 ceramics exhibited a stronger PL intensity than the non-doped one. This suggests that Li-doping in CaF_2 leads to the generation of anion defects, such as F centers, resulting from charge compensation between Ca^{2+} and Li^+. This results in an increase in the number of $(F_2^+)_{Na}$ centers, leading to a stronger PL intensity. Another possibility is that $(F_2^+)_{Li}$ centers, rather than $(F_2^+)_{Na}$ centers adjacent to Na, were formed as $(F_2^+)_A$ centers and contributed to luminescence. Moreover, the generation of $(F_2^+)_{Li}$ centers may have related to the differences in the emission wavelength and spectral shape in comparison with our previous studies [39,42]. In other words, $(F_2^+)_{Li}$ centers are considered to show the differed excitation and emission wavelengths from those of $(F_2^+)_{Na}$ centers. Notably, the PL intensity of the 0.5% Li-doped CaF_2 ceramic was found to be the highest among all the samples studied, and was approximately five times greater than that of the non-doped ceramic.

Figure 5 indicates the RPL dose response function of the 0.5% Li-doped CaF_2 ceramic. This particular ceramic was chosen for analysis due to its high PL intensity. The RPL response was calculated by integrating the PL intensity from 700 to 1000 nm, following ionizing irradiation at varying doses. The linearity of the data was confirmed by performing a least-square fitting with a power function ($y = ax^b$) and determining the coefficient of determination (R^2). The horizontal dashed line indicates the lowest detectable limit of the present reader system, which is expressed as a three-time standard deviation of the instrumental noise (3σ). The minimum detectable doses were estimated from the point of intersection between 3σ and the dose response function. The minimum detectable dose of the 0.5% Li-doped sample turned out to be 14 μGy. It was found that the minimum detectable dose of 0.5% Li-doped CaF_2 was superior to that of the non-doped CaF_2 [39].

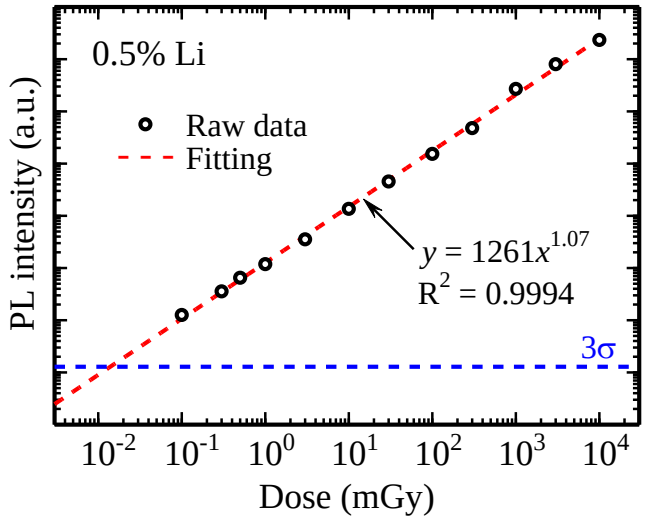

Figure 5. RPL dose response function of the 0.5% Li-doped CaF_2 ceramic.

2.3. Scintillation and TSL Properties

The scintillation spectra of the Li-doped CaF_2 ceramics are displayed in Figure 6. It can be observed that scintillation peaks were consistently observed at around 300 nm in all the samples. This is in line with previous research [46], and the origin of this is self-trapped exciton. In addition, an emission peak at 420 nm was only observed in the 1.0% Li-doped CaF_2 ceramic. The origin of this peak remains unclear; however, a similar peak has been reported in the previous study as well [47].

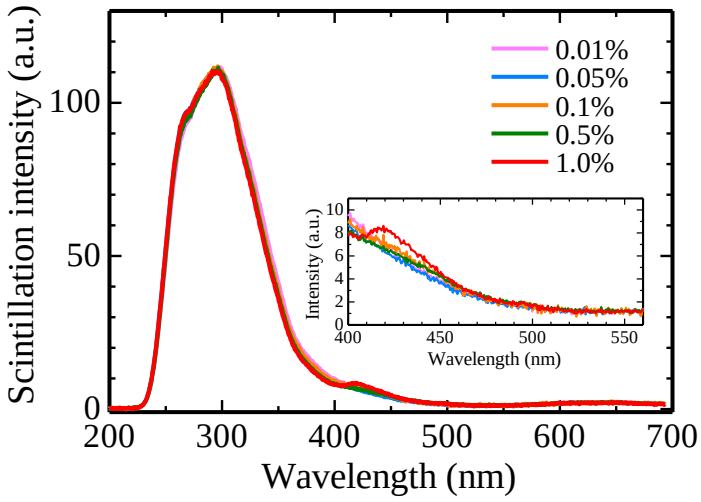

Figure 6. Scintillation spectra of the Li-doped CaF_2 ceramics. The scintillation intensity was normalized.

Figure 7a represents the TSL glow curves of the Li-doped CaF_2 ceramics after X-ray irradiation. All ceramics had a TSL glow peak at around 140 °C with a shoulder shape at 100 °C. The intensity of this peak reached its maximum when the Li-concentration was 0.5%, as was the case with the RPL. Furthermore, a TSL glow peak was detected at temperatures below 50 °C, and a decreasing trend in the intensity was noted as the Li-concentration increased. Figure 7b shows the comparison of the TSL glow curves immediately after ionizing irradiation and 24 h later. The glow peaks at 50 and 100 °C disappeared after one day. In contrast, the glow peak at 140 °C remained relatively unchanged over the same period. The temperature range in which TSL occurred (100–150 °C) was found to be consistent with the bleaching temperature of RPL centers [39]; therefore, this suggests that TSL is a result of the recombination of charge carriers released from RPL centers. However, there is also a possibility that charge carriers released from another (unknown) trap were recombined at the RPL center. Further investigation is needed to establish the relationship between the glow-peak temperature and the bleaching temperature of the RPL centers.

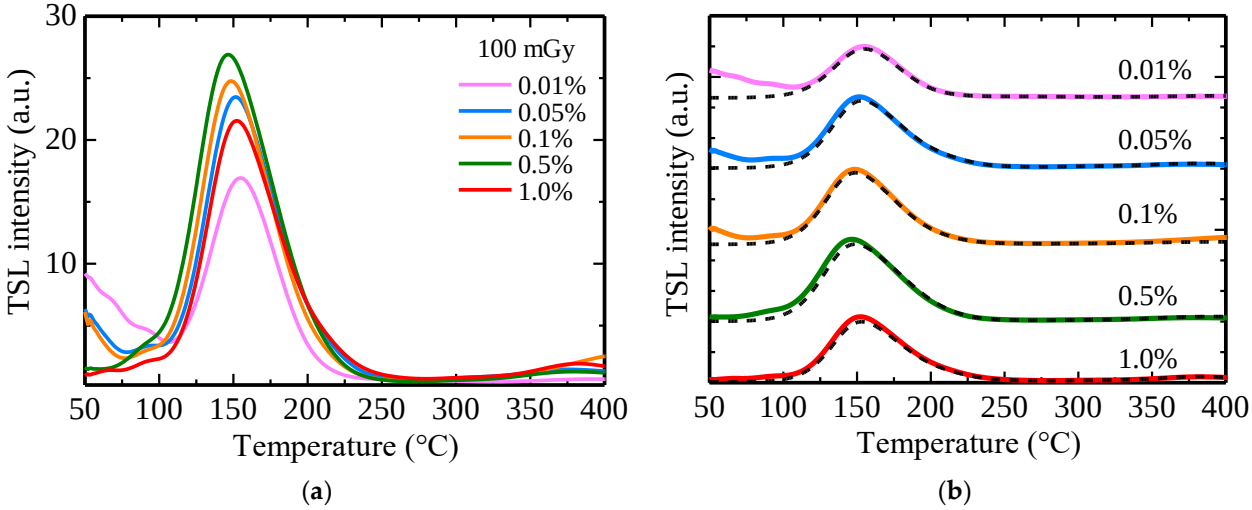

Figure 7. (**a**) TSL glow curves of the Li-doped CaF_2 ceramics. The heating rate was fixed to 1 °C/s. (**b**) Comparison of the TSL glow curves immediately after ionizing irradiation and 24 h later. The black dashed lines show each glow curve 24 h later.

3. Conclusions

This study successfully improved the PL intensity of $(F_2^+)_A$ centers in CaF_2 after ionizing irradiation through Li-doping. The 0.5% Li-doped CaF_2 showed the highest PL intensity among the present samples. Its PL intensity was raised up to five times compared to that of the non-doped CaF_2. This suggests that the presence of Li^+ ions leads to the increase of $(F_2^+)_{Na}$ centers through the generation of anion defects. At the same time, there is a possibility that $(F_2^+)_{Li}$ centers were generated by Li-doping. The RPL intensity of Li-doped CaF_2 was found to be detectable at a low dose of 14 μGy, and continuously increased up to 10 Gy.

Author Contributions: Conceptualization, T.K.; methodology, T.K. and T.Y.; validation, D.N. and N.K.; formal analysis, T.K. and T.Y.; investigation, T.K.; resources, T.K. and T.Y.; data curation, T.K. and N.K.; writing—original draft preparation, T.K.; writing—review and editing, T.K.; visualization, T.K.; supervision, T.Y.; funding acquisition, T.K., D.N., N.K. and T.Y. All authors have read and agreed to the published version of the manuscript.

Funding: This work was supported by Grants-in-Aid for Scientific A (22H00309) and Grants-in-Aid for Scientific B (22H02939, 21H03733, and 21H03736) from Japan Society for the Promotion of Science. The Cooperative Research Project of Research Center for Biomedical Engineering, TEPCO memorial foundation, NAKATANI foundation, and KRF foundation are also acknowledged.

Institutional Review Board Statement: Not applicable.

Informed Consent Statement: Not applicable.

Data Availability Statement: Data of the results presented in this article are not publicly available.

Conflicts of Interest: The authors declare no conflict of interest.

References

1. Okada, G. Novel Radio-Photoluminescence Materials and Applications. *J. Ceram. Soc. Jpn.* **2021**, *129*, 419–424. [CrossRef]
2. Bos, A.J.J. Theory of Thermoluminescence. *Radiat. Meas.* **2006**, *41*, 45–56. [CrossRef]
3. McKeever, S.W.S. Optically Stimulated Luminescence: A Brief Overview. *Radiat. Meas.* **2011**, *46*, 1336–1341. [CrossRef]
4. Bhatt, B.C.; Kulkarni, M.S. Worldwide Status of Personnel Monitoring Using Thermoluminescent (TL), Optically Stimulated Luminescent (OSL) and Radiophotoluminescent (RPL) Dosimeters. *Int. J. Lumin. Appl.* **2013**, *3*, 6–10.
5. Knežević, Ž.; Stolarczyk, L.; Bessieres, I.; Bordy, J.M.; Miljanić, S.; Olko, P. Photon Dosimetry Methods Outside the Target Volume in Radiation Therapy: Optically Stimulated Luminescence (OSL), Thermoluminescence (TL) and Radiophotoluminescence (RPL) Dosimetry. *Radiat. Meas.* **2013**, *57*, 9–18. [CrossRef]
6. Kurobori, T.; Miyamoto, Y.; Maruyama, Y.; Yamamoto, T.; Sasaki, T. A Comparative Study of Optical and Radiative Characteristics of X-Ray-Induced Luminescent Defects in Ag-Doped Glass and LiF Thin Films and Their Applications in 2-D Imaging. *Nucl. Instrum. Methods Phys. Res. Sect. B Beam Interact. Mater. Atoms* **2014**, *326*, 76–80. [CrossRef]
7. Kurobori, T.; Zheng, W.; Miyamoto, Y.; Nanto, H.; Yamamoto, T. The Role of Silver in the Radiophotoluminescent Properties in Silver-Activated Phosphate Glass and Sodium Chloride Crystal. *Opt. Mater.* **2010**, *32*, 1231–1236. [CrossRef]
8. Yamamoto, T.; Maki, D.; Sato, F.; Miyamoto, Y.; Nanto, H.; Iida, T. The Recent Investigations of Radiophotoluminescence and Its Application. *Radiat. Meas.* **2011**, *46*, 1554–1559. [CrossRef]
9. Miyamoto, Y.; Yamamoto, T.; Kinoshita, K.; Koyama, S.; Takei, Y.; Nanto, H.; Shimotsuma, Y.; Sakakura, M.; Miura, K.; Hirao, K. Emission Mechanism of Radiophotoluminescence in Ag-Doped Phosphate Glass. *Radiat. Meas.* **2010**, *45*, 546–549. [CrossRef]
10. Kawamoto, H.; Koshimizu, M.; Fujimoto, Y.; Asai, K. Formation of Radiophotoluminescence Centers at Room Temperature in Ag-Doped Alkali Halides. *Jpn. J. Appl. Phys.* **2019**, *58*, 062004. [CrossRef]
11. Sholom, S.; McKeever, S.W.S. High-Dose Dosimetry with Ag-Doped Phosphate Glass: Applicability Test with Different Techniques. *Radiat. Meas.* **2020**, *132*, 106263. [CrossRef]
12. McKeever, S.W.S.; Sholom, S.; Shrestha, N. Observations Regarding the Build-up Effect in Radiophotoluminescence of Silver-Doped Phosphate Glasses. *Radiat. Meas.* **2019**, *123*, 13–20. [CrossRef]
13. Hashikawa, R.; Fujii, Y.; Kinomura, A.; Saito, T.; Okada, A.; Wakasugi, T.; Kadono, K. Radiophotoluminescence Phenomenon in Copper-Doped Aluminoborosilicate Glass. *J. Am. Ceram. Soc.* **2019**, *102*, 1642–1651. [CrossRef]
14. Asada, S.; Okada, G.; Kato, T.; Nakamura, F.; Kawano, N.; Kawaguchi, N.; Yanagida, T. Eu-Doped Ca_2SiO_4 as a New Radio-Photoluminescence Phosphor. *Chem. Lett.* **2018**, *47*, 59–61. [CrossRef]
15. Calvert, R.L.; Danby, R.J. Thermoluminescence and Radiophotoluminescence from Eu-and Sm-doped $CaSO_4$. *Phys. Status Solidi* **1984**, *83*, 597–604. [CrossRef]

16. Kohara, Y.; Okada, G.; Tsuyumoto, I.; Kusano, E.; Nanto, H. Radiation-Induced Reduction of Eu^{3+} Doped in $SrAl_2O_4$. *Mater. Lett.* **2021**, *303*, 130502. [CrossRef]
17. Dhoble, S.J.; Nagpure, I.M.; Dhoble, N.S.; Molina, P. Effect of Bi Ion on $Eu^{2+} \rightarrow Eu^{3+}$ Conversion in CaF_2:Eu Phosphors for RPL Dosimetry. *J. Mater. Sci.* **2011**, *46*, 7253–7261. [CrossRef]
18. Schuyt, J.J.; Williams, G.V.M. Radiation-Induced Changes in the Optical Properties of $NaMgF_3$(Sm): Observation of Resettable Sm Radio-Photoluminescence. *Mater. Res. Bull.* **2018**, *106*, 455–458. [CrossRef]
19. Okada, G.; Vahedi, S.; Morrell, B.; Koughia, C.; Belev, G.; Wysokinski, T.; Chapman, D.; Varoy, C.; Edgar, A.; Kasap, S. Examination of the Dynamic Range of Sm-Doped Glasses for High-Dose and High-Resolution Dosimetric Applications in Microbeam Radiation Therapy at the Canadian Synchrotron. *Opt. Mater.* **2013**, *35*, 1976–1980. [CrossRef]
20. Chicilo, F.; Okada, G.; Belev, G.; Chapman, D.; Edgar, A.; Curry, R.J.; Kasap, S. Instrumentation for High-Dose, High-Resolution Dosimetry for Microbeam Radiation Therapy Using Samarium-Doped Fluoroaluminate and Fluorophosphate Glass Plates. *Meas. Sci. Technol.* **2020**, *31*, 015201. [CrossRef]
21. Eller, S.A.; Ahmed, M.F.; Bartz, J.A.; Akselrod, M.S.; Denis, G.; Yukihara, E.G. Radiophotoluminescence Properties of Al_2O_3:C,Mg Crystals. *Radiat. Meas.* **2013**, *56*, 179–182. [CrossRef]
22. Akselrod, M.S.; Sykora, G.J. Fluorescent Nuclear Track Detector Technology—A New Way to Do Passive Solid State Dosimetry. *Radiat. Meas.* **2011**, *46*, 1671–1679. [CrossRef]
23. Akselrod, M.S.; Akselrod, A.E. New Al_2O_3:C,Mg Crystals for Radiophotoluminescent Dosimetry and Optical Imaging. *Radiat. Prot. Dosim.* **2006**, *119*, 218–221. [CrossRef]
24. Knežević, Z.; Beck, N.; Milković, D.; Miljanić, S.; Ranogajec-Komor, M. Characterisation of RPL and TL Dosimetry Systems and Comparison in Medical Dosimetry Applications. *Radiat. Meas.* **2011**, *46*, 1582–1585. [CrossRef]
25. Nakamura, F.; Kato, T.; Okada, G.; Kawaguchi, N.; Fukuda, K.; Yanagida, T. Scintillation, TSL and RPL Properties of MgF_2 Transparent Ceramic and Single Crystal. *Ceram. Int.* **2017**, *43*, 7211–7215. [CrossRef]
26. Nakamura, F.; Kato, T.; Okada, G.; Kawano, N.; Kawaguchi, N.; Yanagida, T. Radio-Photoluminescence in Non-Doped K_2CO_3 Ceramics. *Mater. Lett.* **2018**, *211*, 100–102. [CrossRef]
27. Nakamura, F.; Kato, T.; Nakauchi, D.; Okada, G.; Kawano, N.; Kawaguchi, N.; Yanagida, T. Non-Doped Na_2CO_3 Ceramics as a New Radio-Photoluminescence (RPL) Material. *Chem. Lett.* **2017**, *46*, 1383–1385. [CrossRef]
28. Dhopte, S.M.; Muthal, P.L.; Kondawar, V.K. Luminescence in CaF_2:Eu. *J. Lumin.* **1992**, *54*, 95–101. [CrossRef]
29. Bos, A.; Dielhof, J. The Analysis of Thermoluminescent Glow Peaks in CaF_2:Tm (TLD-300). *Radiat. Prot. Dosim.* **1991**, *37*, 231–239. [CrossRef]
30. Danilkin, M.; Lust, A.; Kerikmäe, M.; Seeman, V.; Mändar, H.; Must, M. CaF_2:Mn Extreme Dosimeter: Effects of Mn Concentration on Thermoluminescence Mechanisms and Properties. *Radiat. Meas.* **2006**, *41*, 677–681. [CrossRef]
31. Necmeddin Yazici, A.; Chen, R.; Solak, S.; Yegingil, Z. The Analysis of Thermoluminescent Glow Peaks of CaF_2: Dy (TLD-200) after β-Irradiation. *J. Phys. D. Appl. Phys.* **2002**, *35*, 2526–2535. [CrossRef]
32. Zahedifar, M.; Sadeghi, E. Synthesis and Dosimetric Properties of the Novel Thermoluminescent CaF_2:Tm Nanoparticles. *Radiat. Phys. Chem.* **2012**, *81*, 1856–1861. [CrossRef]
33. Sunta, C.M. Associated Luminescence Centres and Traps in the Thermoluminescence of CaF_2:Dy (TLD-200). *J. Phys. D. Appl. Phys.* **1977**, *10*, 47–51. [CrossRef]
34. Topaksu, M.; Correcher, V.; Garcia-guinea, J. Luminescence Emission of Natural Fluorite and Synthetic CaF_2:Mn. *Radiat. Phys. Chem.* **2016**, *119*, 151–156. [CrossRef]
35. Bakshi, A.K.; Dhabekar, B.; Rawat, N.S.; Singh, S.G.; Joshi, V.J.; Kumar, V. Study on TL and OSL Characteristics of Indigenously Developed CaF_2:Mn Phosphor. *Nucl. Instrum. Methods Phys. Res. Sect. B Beam Interact. Mater. Atoms* **2009**, *267*, 548–553. [CrossRef]
36. Asfora, V.; De Barros, V.S.M.; Da Silva, R.J.G.; Vasconcelos, D.A.A.; Nobre, B.S.; Yamato, M.E.; Khoury, H.J.; Oliveira, R.A.; Azevedo, W.M. Optically Stimulated Luminescence of CaF_2:Tm. *Radiat. Meas.* **2016**, *85*, 73–77. [CrossRef]
37. Nakamura, F.; Kato, T.; Okada, G.; Kawaguchi, N.; Fukuda, K.; Yanagida, T. Scintillation and Dosimeter Properties of CaF_2 Transparent Ceramic Doped with Eu^{2+}. *Ceram. Int.* **2017**, *43*, 604–609. [CrossRef]
38. Kato, T.; Nakauchi, D.; Kawaguchi, N.; Yanagida, T. Radio-Photoluminescence Phenomenon in Non-Doped CaF_2 Ceramic. *Mater. Lett.* **2020**, *270*, 127688. [CrossRef]
39. Kato, T.; Nakauchi, D.; Kawaguchi, N.; Yanagida, T. Radio-Photoluminescence Properties of CaF_2 Transparent and Opaque Ceramics. *Curr. Appl. Phys.* **2020**, *20*, 1195–1200. [CrossRef]
40. Tijero, J.M.G.; Jaque, F. Thermal and Optical Properties of the F_A and $(F_2^+)_A$ Centers in Na-Doped CaF_2 Crystals. *Phys. Rev. B* **1990**, *41*, 3832–3836. [CrossRef]
41. Komine, N.; Sakuma, S.; Shiozawa, M.; Mizugaki, T.; Sato, E. Influence of Sodium Impurities on ArF Excimer-Laser-Induced Absorption in CaF_2 Crystals. *Appl. Opt.* **2000**, *39*, 3925–3930. [CrossRef]
42. Kato, T.; Okada, G.; Nakauchi, D.; Kawaguchi, N.; Yanagida, T. Na-Concentration Dependence on Radiophotoluminescence Properties of CaF_2. *Solid State Sci.* **2022**, *128*, 106892. [CrossRef]
43. Yanagida, T.; Kamada, K.; Fujimoto, Y.; Yagi, H.; Yanagitani, T. Comparative Study of Ceramic and Single Crystal Ce:GAGG Scintillator. *Opt. Mater.* **2013**, *35*, 2480–2485. [CrossRef]
44. Yanagida, T.; Fujimoto, Y.; Kawaguchi, N.; Yanagida, S. Dosimeter Properties of AlN. *J. Ceram. Soc. Japan* **2013**, *121*, 988–991. [CrossRef]

45. Kato, T.; Shiratori, D.; Nakauchi, D.; Kawaguchi, N.; Yanagida, T. Evaluation of Quantum Yields and Thermally Stimulated Luminescence Glow Curves of Ag-Doped Phosphate Glasses. *Jpn. J. Appl. Phys.* **2020**, *59*, 112001. [CrossRef]
46. Cramer, L.P.; Cumby, T.D.; Leraas, J.A.; Langford, S.C.; Dickinson, J.T. Effect of Surface Treatments on Self-Trapped Exciton Luminescence in Single-Crystal CaF_2. *J. Appl. Phys.* **2005**, *97*, 103533. [CrossRef]
47. Antonyak, O.T.; Vistovskyy, V.V.; Zhyshkovych, A.V.; Kravchuk, I.M. Defect Luminescence in CaF_2 Nanoparticles. *J. Lumin.* **2015**, *167*, 249–253. [CrossRef]